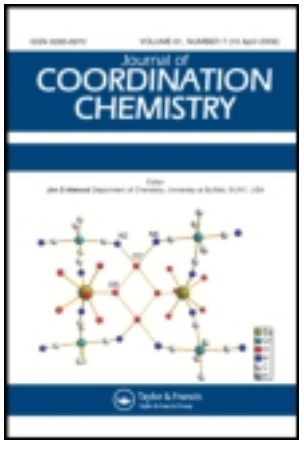

Journal of Coordination Chemistry
Publication details, including instructions for authors and subscription information:
http://www.tandfonline.com/loi/gcoo20

Synthesis, thermal and spectroscopic properties, and crystal structures of $[Co(bba)_2(H_2O)(phen)]$ and $[Ni(bba)_2(H_2O)(butOH)(phen)]$ (bba=2-benzoylbenzoate, phen=1,10-phenanthroline, butOH=butanol)

Sema Caglar [a], Zerrin Heren [b] & Orhan Büyükgüngör [c]
[a] Department of Chemistry, Faculty of Arts and Sciences, Erzincan University, 24100, Erzincan, Turkey
[b] Department of Chemistry, Faculty of Arts and Sciences, Ondokuz Mayis University, 55139, Kurupelit, Samsun, Turkey
[c] Department of Physics, Faculty of Arts and Sciences, Ondokuz Mayis University, 55139, Kurupelit, Samsun, Turkey
Published online: 08 Apr 2011.

To cite this article: Sema Caglar, Zerrin Heren & Orhan Büyükgüngör (2011) Synthesis, thermal and spectroscopic properties, and crystal structures of $[Co(bba)_2(H_2O)(phen)]$ and $[Ni(bba)_2(H_2O)(butOH)(phen)]$ (bba=2-benzoylbenzoate, phen=1,10-phenanthroline, butOH=butanol), Journal of Coordination Chemistry, 64:7, 1289-1298

To link to this article: http://dx.doi.org/10.1080/00958972.2011.566923

Journal of Coordination Chemistry
Vol. 64, No. 7, 10 April 2011, 1289–1298

Synthesis, thermal and spectroscopic properties, and crystal structures of $[Co(bba)_2(H_2O)(phen)]$ and $[Ni(bba)_2(H_2O)(butOH)(phen)]$ (bba = 2-benzoylbenzoate, phen = 1,10-phenanthroline, butOH = butanol)

SEMA CAGLAR*†, ZERRIN HEREN‡ and ORHAN BÜYÜKGÜNGÖR§

†Department of Chemistry, Faculty of Arts and Sciences,
Erzincan University, 24100, Erzincan, Turkey
‡Department of Chemistry, Faculty of Arts and Sciences,
Ondokuz Mayis University, 55139, Kurupelit, Samsun, Turkey
§Department of Physics, Faculty of Arts and Sciences,
Ondokuz Mayis University, 55139, Kurupelit, Samsun, Turkey

(*Received 3 November 2010; in final form 4 February 2011*)

Aquabis(2-benzoylbenzoato)(1,10-phenanthroline)cobalt(II) and aquabis(2-benzoylbenzoato)(butanol)(1,10-phenanthroline)nickel(II) have been prepared and characterized by elemental analyses, IR and electronic spectroscopy, magnetic measurements, and single-crystal X-ray diffraction. $[Co(bba)_2(H_2O)(phen)]$ (**1**) and $[Ni(bba)_2(H_2O)(butOH)(phen)]$ (**2**) consist of neutral monomeric units and crystallize in the monoclinic ($P2(1)$) and triclinic ($P\bar{1}$) crystal systems, respectively. The cobalt(II) and nickel(II) sit on inversion centres and exhibit distorted octahedral coordination. Phen is bidentate chelating. In **1**, bba is both monodentate and bidentate, whereas in **2** bba is only monodentate. bba ligands are coordinated to metal(II) with carboxylates and IR spectra of both complexes display characteristic absorptions of carboxylate anions $\{\nu(OCO)_{asym}$ and $\nu(OCO)_{sym}\}$ of bba. Thermal analysis shows that mass losses of **1** from 105°C to 456°C correspond to decomposition of phen and bba, while for **2** these occur at 271–529°C.

Keywords: 2-Benzoylbenzoic acid; 1,10-Phenanthroline; Cobalt(II) complex; Nickel(II) complex; Crystal structure

1. Introduction

Carboxylate ligands are among the most widely studied ligand classes providing compounds with interesting topologies. Versatile coordination modes are available with carboxylates, monodentate, chelate, different types of CO_2 bridges, and monoatomic bridges [1] and also stable complexes of low coordination numbers could be available by flexible and sterically bulky ligands. Hybrid porous solids such as metal–organic framework materials produced by carboxylate derivatives with metal salts have

*Corresponding author. Email: semacaglar2002@hotmail.com

Journal of Coordination Chemistry
ISSN 0095-8972 print/ISSN 1029-0389 online © 2011 Taylor & Francis
DOI: 10.1080/00958972.2011.566923

applications in many fields due to their high surface area, porosity, and attractive adsorptive properties [2–5]. 2-Benzoylbenzoic acid (Hbba) and its derivatives are used in the synthesis of supramolecular coordination compounds [6] for electron-transport materials [6] and sweeteners [7]. Although the crystal structure of 2-benzoylbenzoic acid (Hbba = $C_{14}H_{10}O_3$, also named *o*-benzoylbenzoic acid) was investigated in 1990 [8], only a limited number of articles relating to 2-benzoylbenzoate [bba = $(C_{14}H_9O_3)^-$] complexes have been published [6–15]. bba is a versatile polyfunctional ligand, due to the presence of the negatively charged carboxylate and carbonyl oxygens.

As a part of our study on the synthesis, spectral and thermal analysis of transition metal complexes of bba with phen, as co-ligand, in this study we report the synthesis, spectral and thermal characterization, and crystal structures of $[Co(bba)_2(H_2O)(phen)]$ (**1**) and $[Ni(bba)_2(H_2O)(butOH)(phen)]$ (**2**).

2. Experimental

2.1. *Methods of sample characterization*

All reactions were performed with commercially available reagents, used without purification, and the solvents were distilled and dried by standard procedures. IR spectra were recorded on a Bruker Vertex 80 V FT-IR spectrophotometer from 4000 to 450 cm^{-1} at 4 cm^{-1} resolution using KBr pellets. Electronic spectra were measured on a Unicam UV2 from 200 to 900 nm in MeOH. The C, H, and N contents were determined with an Elementar Micro Vario CHNS. Room temperature magnetic susceptibility measurements were carried out using a Sherwood Scientific MXI model Evans magnetic balance. Thermal analysis curves (TG, DTA, DTG) were obtained simultaneously on a Perkin-Elmer Diamond thermal analyzer in static air. Samples of 5–10 mg were used.

2.2. *Synthesis of $[Co(bba)_2(H_2O)(phen)]$ (1)*

2-Hbba (2-benzoylbenzoic acid) ligand (0.136 g, 0.6 mmol) and $Co(CH_3COO)_2 \cdot 4H_2O$ (0.075 g, 0.3 mmol) were dissolved in MeOH (40 cm^3) with continuous stirring at 100°C. The protonation of acetate by Hbba resulted in the formation of bba. Then phen (0.054 g, 0.3 mmol) dissolved in MeOH (5 cm^3) was added dropwise to the first solution. X-ray quality pink crystals of $[Co(bba)_2(H_2O)(phen)]$ were obtained by slow evaporation of the solution at room temperature after 1 week. Yield: 80%; m.p.: 97°C. Anal. Calcd for $C_{40}H_{28}N_2O_7Co$ (%): C, 67.89; H, 3.96; N, 3.9. Found (%): C, 67.80; H, 3.84; N, 3.90.

2.3. *Synthesis of $[Ni(bba)_2(H_2O)(butOH)(phen)]$ (2)*

2-Hbba (0.136 g, 0.6 mmol) and $Ni(CH_3COO)_2 \cdot 4H_2O$ (0.075 g, 0.3 mmol) were dissolved in butanol–ethanol (butOH–EtOH) (mixture (1 : 1); 40 cm^3) with continuous stirring at 100°C. The protonation of acetate by Hbba resulted in the formation of bba. Then a solution of phen (0.054 g, 0.3 mmol) in MeOH (5 cm^3) was added to the

first solution. Green crystals of [Ni(bba)$_2$(H$_2$O)(butOH)(phen)] were obtained by slow evaporation at room temperature after 1 week. Yield: 75%; m.p.: 111°C. Anal. Calcd for $C_{44}H_{38}N_2O_8Ni$ (%): C, 67.63; H, 4.86; N, 3.58. Found (%): C, 67.48; H, 4.7; N, 3.46.

2.4. *X-ray crystallography*

Intensity data for **1** and **2** were collected using a STOE IPDS-II area detector diffractometer (Mo-Kα radiation, $\lambda = 0.71073$ Å) at 293 K. The structures were solved by direct methods and refined on F^2 with SHELX-97 [16]. All non-hydrogen atoms were refined with anisotropic parameters. All hydrogens were included using a riding model. The details of data collection, refinement, and crystallographic data are summarized in table 1.

3. Results and discussion

3.1. *IR spectra*

Selected IR bands of Hbba, **1** and **2** are listed in table 2. Sharp bands at 3447–3562 cm^{-1} are attributed to ν(OH) of aqua ligand. The relatively weak bands at 3054–3059 cm^{-1}

Table 1. Crystal data and structure refinement parameters for **1** and **2**.

	1	**2**
Empirical formula	$C_{40}H_{28}N_2O_7Co$	$C_{44}H_{38}N_2O_8Ni$
Formula weight	707.57	781.45
Temperature (K)	293	293
Wavelength (Å)	0.71073	0.71073
Crystal system	Monoclinic	Triclinic
Space group	*P2(1)*	*P*$\bar{1}$
Unit cell dimensions (Å, °)		
a	8.5242(4)	10.1419(3)
b	22.5543(9)	13.3548(4)
c	8.9758(4)	15.7023(5)
α	90	72.715(2)
β	109.098(4)	71.830(2)
γ	90	88.490(2)
Volume (Å)^3, *Z*	1630.68(12), 2	1924.30(10), 2
Calculated density (Mg m^{-3})	1.441	1.349
Absorption coefficient (mm^{-1})	0.58	0.561
Crystal size (mm^3)	0.340 × 0.513 × 0.610	0.190 × 0.387 × 0.720
θ range for data collection (°)	1.81–26.50	1.43–26.50
Measured reflections	13,297	31,628
Independent reflections	6652	7984
Absorption correction[a]	Integration	Integration
Refinement method	Full-matrix least-squares on F^2	Full-matrix least-squares on F^2
Goodness-of-fit on F^2	0.967	1.047
Final *R* indices [$F^2 > 2\sigma(F^2)$]	0.0380	0.0526
Largest difference peak and hole (e Å^{-3})	0.33, −0.39	0.66, −0.42

[a]Stoe & Cie [17].

Table 2. Selected IR spectral data for Hbba, **1**, and **2**.[a]

	Hbba	**1**	**2**
ν(OH)	3445 m	3520 m	3447 m
ν_{aro}(CH)	3060w	3054w	3059w
ν_{alf}(CH)	–	–	2920–2866w
ν(C=O)	1673vs	1666vs	1676vs
$\nu_{asym}(COO^-)$	–	1542s	1546s
$\nu_{sym}(COO^-)$	–	1386vs	1386vs

w, weak; m, medium; s, strong; vs, very strong.
[a]Frequencies in cm^{-1}.

are due to aromatic ν(CH) and weak bands at 2866–2955 cm^{-1} are assigned to aliphatic ν(CH) of butOH ligand. Absorptions of the carbonyl of bba in the complexes are observed at 1666 and 1676 cm^{-1}. Carboxylate anions have typical $\nu(OCO)_{asym}$ {1542 cm^{-1} for **1**, 1546 cm^{-1} for **2**} and $\nu(OCO)_{sym}$ {1386 cm^{-1} for **1**, 1386 cm^{-1} for **2**}. The calculated Δ(OCO) values $\{\nu(OCO)_{asym} - \nu(OCO)_{sym}\}$ of 156 cm^{-1} **1** and 160 cm^{-1} **2** are lower than the values expected for monodentate carboxylate (>200 cm^{-1}) but reduction in Δ(OCO) values are typical where such carboxylates are involved in hydrogen bonding [18]. Bands around 1581 cm^{-1} correspond to ν(C=C) of bba and phen ligands; the bands at around 1250–1320 cm^{-1} are due to ν(C–O) vibration.

3.2. *UV-Vis spectra and magnetic properties*

Electronic spectra of both complexes are prepared in MeOH; **1** shows only two bands with low intensity centered at 475 nm ($\varepsilon = 17\,dm^3\,mol^{-1}\,cm^{-1}$) and 499 nm ($\varepsilon = 19\,dm^3\,mol^{-1}\,cm^{-1}$) due to d–d transitions and a third band also appears at *ca* 950 nm from the shape of the spectra of the complex. Complex **2** exhibits three maxima at 410 nm ($\varepsilon = 12\,dm^3\,mol^{-1}\,cm^{-1}$), 601 nm ($\varepsilon = 6\,dm^3\,mol^{-1}\,cm^{-1}$), and 865 nm ($\varepsilon = 4\,dm^3\,mol^{-1}\,cm^{-1}$). Intense bands at 220–300 nm are assigned to ligand-centered (*L–L**) transition with bba and phen.

Magnetic susceptibility measurements indicate that cobalt(II) complexes exhibit high spin d^7 configurations. The effective magnetic moments of **1** and **2** at room temperature are 4.45 and 2.69 B.M., respectively, consistent with the calculated values (3.87 and 2.83 B.M., respectively) of the spin-only magnetic moment of the octahedral coordination geometry around cobalt(II) and nickel(II).

3.3. *Thermal analysis*

Thermal behavior of **1** and **2** were followed to 900°C in static air. Complex **1** decomposes in three stages. The first between 74°C and 105°C corresponds to endothermic dehydration with a mass loss of 3.5% (Calcd 2.5%). After dehydration, the anhydrous complex begins to decompose with melting at 284°C (DTA curve). Degradation of one phen and decomposition of the two bba ligands take place in the second (105–368°C) and third stage (368–456°C) with a mass loss of 88.22% (Calcd 86.87%). The last mass loss of the complex is vigorous and strongly exothermic (DTA at 432°C) and related to the burning organic residue. Mass-loss calculations suggest

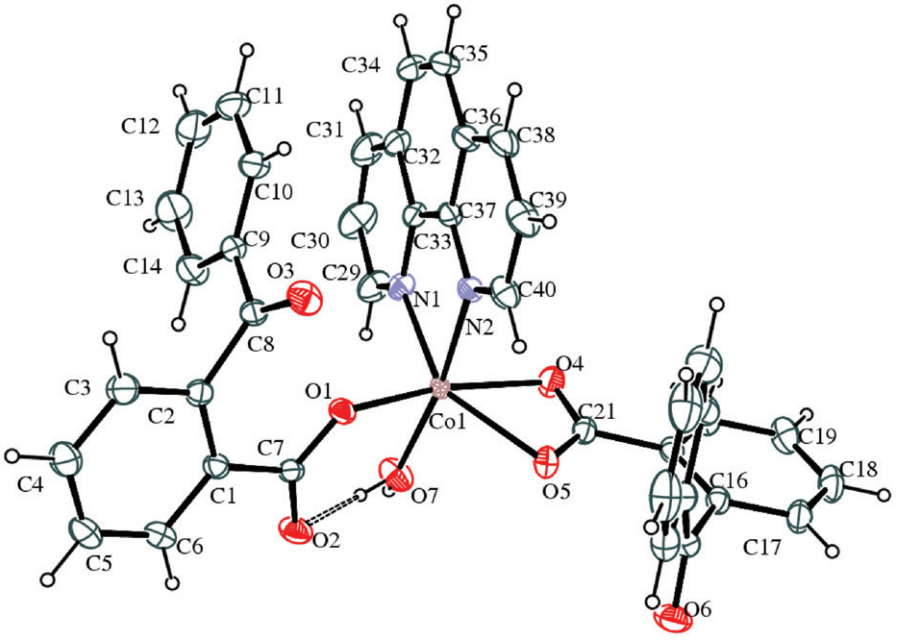

Figure 1. ORTEP III diagram and atom-numbering scheme of **1**. The hydrogen bond is drawn as dashed lines. Displacement ellipsoids are drawn at the 20% probability level.

that the product at 457°C is Co_3O_4, which further decomposes to the end product CoO at 890°C.

Complex **2** displays a similar thermal reactivity beginning with endothermic dehydration and elimination of butOH with a mass loss of 11.49% (Calcd 11.77%) (96–271°C). Then $[Ni(bba)_2(phen)]$ begins to decompose, melting at 280°C (DTA curve) through elimination of one phen and one bba at 271–308°C. The experimental mass loss of 50.17% agrees with the calculated mass loss of 51.87%. From 308°C to 529°C, decomposition of the bba proceeds, extremely exothermic (DTA at 471°C) and related to the burning organic residue (Found 28.27%; Calcd 28.83%). The final product is NiO (Found 90.11%; Calcd 90.44%).

3.4. *Crystal structure of 1*

The molecular structure of $[Co(bba)_2(H_2O)(phen)]$ with atom labeling is shown in figure 1. Selected bond lengths and angles together with hydrogen-bonding geometry are listed in table 3. The structure consists of individual molecules of **1**, in which cobalt(II) is coordinated by one aqua, one phen, and two bba, forming octahedral CoN_2O_4. Bba occupy the *trans* positions of the octahedron. Phen is bidentate, while bba are both monodentate and bidentate occupying the equatorial plane of the coordination octahedron.

The $Co–N_{phen}$ bond distances are 2.101(2)–2.130(2) Å and a N–Co–N chelating angle [78.21(8)°] similar to other reported for $[Co(bpo)_2(phen)]$ [2.143–2.149 Å; 78.0°] [19] $K[Co(phen)_2(H_2O)]_2[HCoW_{12}O_{40}]\cdot 2H_2O$ [2.112(17)–2.16(2) Å; 78.5(7)°] [20],

Table 3. Selected geometric parameters and hydrogen bonds (Å, °) for **1**.

Co1–N1	2.101(2)	Co1–O4	2.1366(18)
Co1–N2	2.130(2)	Co1–O5	2.2238(17)
Co1–O1	2.0437(16)	Co1–O7	2.112(2)
O1–Co1–N1	102.54(8)	O4–Co1–N2	94.45(8)
O1–Co1–N2	85.70(7)	O5–Co1–O7	95.19(8)
O1–Co1–O4	167.72(7)	O5–Co1–N1	147.34(7)
O1–Co1–O5	107.56(7)	O5–Co1–N2	91.53(7)
O1–Co1–O7	88.77(8)	O7–Co1–N1	97.88(9)
O4–Co1–O5	60.16(7)	O7–Co1–N2	172.34(9)
O4–Co1–O7	92.08(9)	N2–Co1–N1	78.21(8)
O4–Co1–N1	89.49(8)		

Hydrogen bonds D–H···A	D–H (Å)	H···A (Å)	D···A (Å)	D–H···A (°)
O7–H7A···O2	0.78(5)	1.83(5)	2.58(3)	159(5)

$[Co^{II}(phen)\{3,5\text{-}(NO_2)_2sal^{2-}\}]_n$ [2.112(4)–2.134(4) Å; 78.32(16)°] [21], $[Co(phen)(H_2O)(VO)(H_2O)(HPO_4)_2]$ [2.067(3)–2.119(2) Å; 78.92(9)°] [22], and $[Co(phen)_2(H_2O)_2]sac_2 \cdot H_2O$ [2.118(2)–2.164(2) Å; 77.91(8)°–78.24(8)°] [23], where bpo, $3,5\text{-}(NO_2)_2sal^{2-}$, and sac are 2-OH-benzophenones, 3,5-dinitrosalicylate anion, and saccharinate, respectively. The *cis*-angles range from 60.16(7)° to 102.54(8)° and indicate a significant distortion of the coordination polyhedron. There is an intramolecular hydrogen bond between the hydrogen of aqua and carboxylate of bba (table 3). There are C3–H3···Cg5 (C15–C20) interactions between the phenyl rings of bba (2.75 Å) and C27–H27···Cg7 (C32–C37) interactions between the phenyl rings of bba and phen (2.75 Å) (figure 2).

3.5. *Crystal structure of 2*

The molecular structure of $[Ni(bba)_2(H_2O)(butOH)(phen)]$ consist of neutral molecules (figure 3). Selected bond lengths and angles together with hydrogen-bonding geometry are collected in table 4. The nickel(II) is coordinated by one aqua, one butOH, one phen, and two bba, exhibiting a distorted octahedral configuration, NiN_2O_4. The phen is bidentate *via* two nitrogens, creating a five-membered chelate ring, while the two bba are monodentate through oxygen.

$Ni–N_{phen}$ bond distances of 2.0761(18)−2.0813(18) Å are comparable to distances found in $[Ni(phen)_2(1,3\text{-dtsq})]$ [24], $[Ni(phen)_2(1,2\text{-dtsq})] \cdot 3.5H_2O$ [25], $[Ni(pao)_2(phen)]$ [24], and $[Ni(phen)(H_2O)(VO)(H_2O)(HPO_4)_2]$ [22], where dtsq and pao are dithiosquarate and pyridine-2-aldoximate, respectively. $Ni–O_{bba}$ bond distances are 2.0653(15) and 2.0996(14) Å, slightly shorter than the corresponding values in $[Ni(bba)_2(et)_2(imidazol)_2]$ [14]. Distortions in the coordination polyhedral from ideal octahedral geometry are also clearly evident from the *cis* angles, which are from 79.79(8)° to 96.50(7)°. There is a strong intramolecular hydrogen bond between hydrogen of aqua

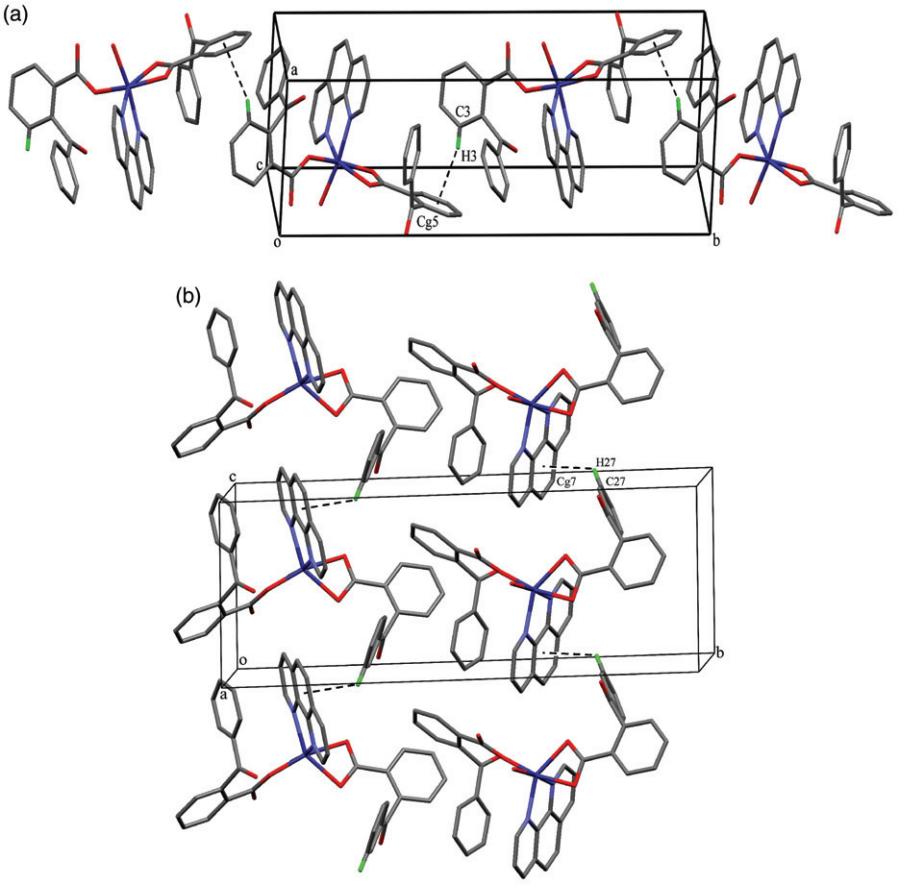

Figure 2. (a, b) A crystal packing diagram of **1**, viewed along the *b*-axis, showing C–H $\cdots\pi$ interaction.

and carboxylate of bba (table 4). Additionally, there are C–H $\cdots\pi$ interactions [C40–H40 $\cdots$ Cg3 (N2, C7–C11) and C39–H39 $\cdots$ Cg5 (C21–C26)] between the phenyl rings of bba and phen (2.98 Å) and the phenyl rings of bba ligands (2.87 Å), respectively (figure 4).

4. Conclusions

The Co(II) and Ni(II) complexes have been characterized by elemental analyses, magnetic moments, UV-Vis, FT-IR, thermal analyses, and X-ray diffraction. X-ray crystal structure analysis showed that **1** and **2** consist of neutral monomeric units. The cobalt(II) and nickel(II) sit on inversion centres and exhibit distorted octahedral coordination. The hydrogen of aqua ligand is involved in intramolecular hydrogen

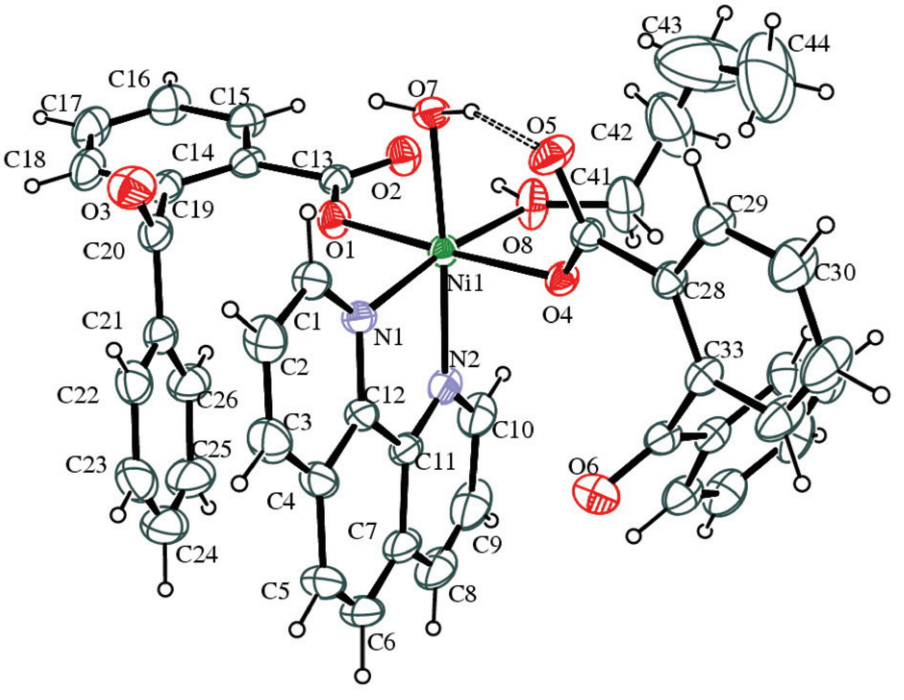

Figure 3. ORTEP III diagram and atom-numbering scheme of **2**. The hydrogen bond is indicated by dashed lines. Displacement ellipsoids are drawn at the 20% probability level.

Table 4. Selected geometric parameters and hydrogen bonds (Å, °) for **2**.

Ni1–N1	2.0813(18)	Ni1–O4	2.0996(14)	
Ni1–N2	2.0761(18)	Ni1–O7	2.0783(15)	
Ni1–O1	2.0653(15)	Ni1–O8	2.0593(19)	
O1–Ni1–O4	177.66(6)	O4–Ni1–N2	91.00(6)	
O1–Ni1–O7	86.86(7)	O7–Ni1–O8	89.77(9)	
O1–Ni1–O8	89.93(7)	O7–Ni1–N1	96.50(7)	
O1–Ni1–N1	94.50(7)	O7–Ni1–N2	175.64(8)	
O1–Ni1–N2	91.14(7)	O8–Ni1–N1	172.51(8)	
O4–Ni1–O7	91.06(6)	O8–Ni1–N2	94.10(10)	
O4–Ni1–O8	89.00(7)	N2–Ni1–N1	79.79(8)	
O4–Ni1–N1	86.80(6)			
Hydrogen bonds				
D–H···A	D–H (Å)	H···A (Å)	D···A (Å)	D–H···A (°)
O7–H7B···O5	0.85(2)	1.79(2)	2.60(2)	159(3)

bond with carboxylate oxygen of bba for **1** and **2**. Additionally, the chains are cross linked by C–H···π interactions. The magnetic susceptibility measurements show that **1** is high spin d^7. Thermal analysis data for **1** demonstrated mass losses at 75–105°C, 105–368°C, and 368–456°C, which correspond to decomposition of aqua, phen, and bba, respectively, while **2** shows mass losses at 96–271°C, 271–308°C, and 308–529°C due to the aqua-ButOH, phen-bba, and bba, respectively.

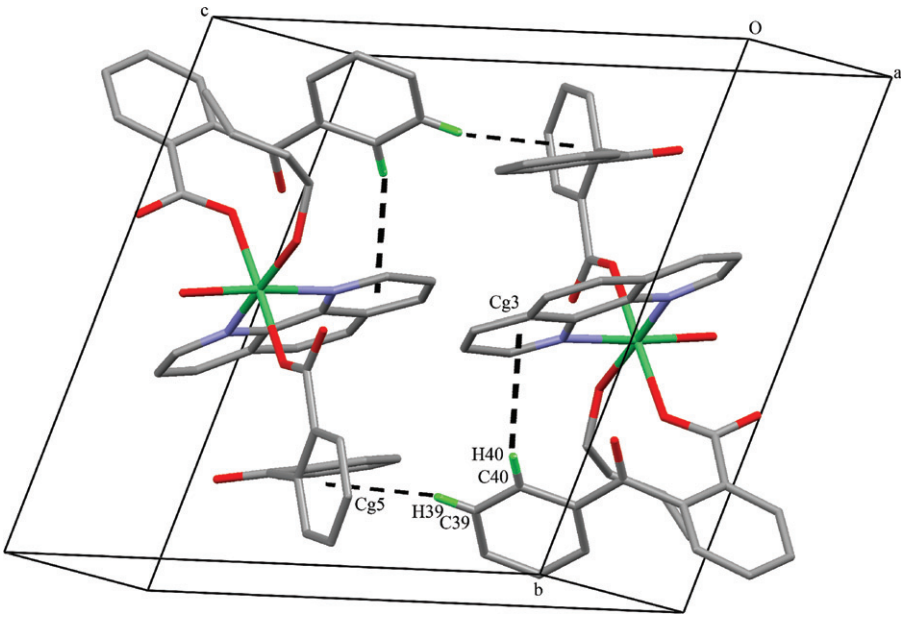

Figure 4. A crystal packing diagram of **2** showing C–H $\cdots\pi$ interaction.

Supplementary material

Crystallographic data for structural analysis have been deposited with the Cambridge Crystallographic Data Center, CCDC no. 789651 for **1** and CCDC no. 789650 for **2**. Copies of these information may be obtained free of charge from The Director, CCDC, 12 Union Road, Cambridge CB2 1EZ, UK (Fax: +44 1223 336033; E-mail: deposit@ccdc.cam.ac.uk or www: http://www.ccdc.cam.ac.uk).

References

[1] R. Baggio, R. Calvo, M.T. Garland, O. Peña, M. Perec, L.D. Slep. *Inorg. Chem. Commun.*, **10**, 1249 (2007).
[2] M. Eddaoudi, D.B. Moler, H. Li, B. Chen, T.M. Reineke, M. O'Keeffe, O. Yaghi. *Acc. Chem. Res.*, **34**, 319 (2001).
[3] J. Moellmer, E.B. Celer, R. Luebke, A.J. Cairns, R. Staudt, M. Eddaoudi, M. Thommes. *Microporous Mesoporous Mater.*, **129**, 345 (2010).
[4] H. Li, M. Eddaoudi, M. O'Keeffe, O.M. Yaghi. *Nature*, **402**, 276 (1999).
[5] H. Furukawa, M.A. Miller, O.M. Yaghi. *J. Mater. Chem.*, **17**, 3197 (2007).
[6] D. Wang, H. Zhu, N. Shan, G. Song, J. Wang. *Acta Cryst.*, **E62**, 304 (2006).
[7] A. Arnoldi, A. Bassoli, G. Borgonovo, L. Merlini, G. Morini. *J. Agric. Food Chem.*, **45**, 2047 (1997).
[8] R.A. Lalencette, P.A. Vanderhoff, H.W. Thompson. *Acta Cryst.*, **C46**, 1682 (1990).
[9] M.R.J. Foreman, M.J. Plater, J.M.S. Skakle. *J. Chem. Soc., Dalton Trans.*, 1897 (2001).
[10] Y. Song, B. Yan, Z. Chen. *J. Coord. Chem.*, **58**, 1417 (2005).
[11] C.A.K. Diop, A. Toure, L. Diop, R. Welter. *Acta Cryst.*, **E62**, m3338 (2006).
[12] L. Liu, Z. Xu, Z. Lou, F. Zhang, B. Sun, J. Pei. *J. Rare Earths*, **24**, 253 (2006).
[13] L. Liu, Z. Xu, Z. Lou, F. Zhang, B. Sun, J. Pei. *J. Luminescence*, **122–123**, 961 (2007).
[14] Z. Heren, H. Paşaoğlu, M.H. Yıldırım, D. Hıra. *Acta Cryst.*, **E65**, 907 (2009).
[15] M.H. Yıldırım, Z. Heren, H. Paşaoğlu, D. Hıra, O. Büyükgüngör. *Acta Cryst.*, **E65**, 638 (2009).

[16] G.M. Sheldrick. *Acta Cryst.*, **A64**, 112 (2008).
[17] Stoe & Cie. *X-AREA (Version 1.18)* and *X-RED32 (Version 1.04)*, Stoe & Cie, Darmstadt, Germany (2002).
[18] M. Devereux, M. McCann, V. Leon, R. Kelly, D.O. Shea, V. McKee. *Polyhedron*, **22**, 3187 (2003).
[19] C.D. Papadopoulos, A.G. Hatzidimitriou, M. Quirós, M.P. Sigalas, M. Lalia-Kantouri. *Polyhedron*, **30**, 486 (2011).
[20] J. Sha, J. Peng, J. Chen, H. Liu, A. Tian, P. Zhang. *Solid State Sci.*, **9**, 1012 (2007).
[21] X. He, Y.-N. Li, G.-H. Li, Y.-Z. Li, P. Zhang, J.-N. Xu, Y. Wang. *Inorg. Chem. Commun.*, **8**, 983 (2005).
[22] Y. Cui, Y. Xing, G. Li, Y. Liu, H. Meng, L. Liu, W. Pang. *J. Solid State Chem.*, **177**, 3080 (2004).
[23] A.S. Batsanov, C. Bilton, R.M.K. Deng, K.B. Dillon, A.E. Goeta, J.A.K. Howard, H.J. Shepherd, S. Simon, I. Tembwe. *Inorg. Chim. Acta*, **365**, 225 (2011).
[24] H. Miyasaka, S. Furukawa, S. Yanagida, K. Sugiura, M. Yamashita. *Inorg. Chim. Acta*, **357**, 1619 (2004).
[25] M.T. Calatayud, J. Sletten, I. Castro, M. Julve, G. Seitz, K. Mann. *Inorg. Chim. Acta*, **353**, 159 (2003).